Stochastic Models for Circadian Oscillations: Emergence of a Biological Rhythm

DIDIER GONZE, JOSÉ HALLOY, ALBERT GOLDBETER

Unité de Chronobiologie Théorique, Faculté des Sciences, Université Libre de Bruxelles, Campus Plaine, C. P. 231, B-1050 Brussels, Belgium

Received 26 March 2003; accepted 27 October 2003
Published online 14 January 2004 in Wiley InterScience (www.interscience.wiley.com).
DOI 10.1002/qua.10875

ABSTRACT: Nearly all living organisms display circadian oscillations characterized by a period close to 24 h. These rhythms originate from the negative autoregulation of gene expression. Deterministic models based on such genetic regulatory processes account for the occurrence of circadian rhythms in constant environmental conditions (e.g., constant darkness), for entrainment of these rhythms by light–dark cycles, and for their phase-shifting by light pulses. When the numbers of protein and mRNA molecules involved in the oscillations are small, as may occur in cellular conditions, it becomes necessary to resort to stochastic simulations to assess the influence of molecular noise on circadian oscillations. We address the effect of molecular noise by considering the stochastic version of a core deterministic model previously proposed for circadian oscillations of the PER protein and its mRNA in *Drosophila*. The model is based on cooperative repression of the *per* gene by the PER protein. Numerical simulations of the stochastic version of the model are performed by means of the Gillespie method. The predictions of the stochastic approach compare well with those of the deterministic model with respect to both sustained oscillations of the limit cycle type and the influence of the proximity from a bifurcation point below which the system evolves to a stable steady state. Stochastic simulations indicate that robust circadian oscillations can emerge at the cellular level, even when the maximum numbers of mRNA and protein molecules involved in the oscillations are of the order of only a few tens or hundreds. The stochastic simulations also reproduce the evolution toward a strange attractor in conditions where an extended version of the deterministic model admits chaotic

Correspondence to: Albert Goldbeter; e-mail: agoldbet@ulb.ac.be

Contract grant sponsor: Fonds de la Recherche Scientifique Médicale (F. R. S. M., Belgium).
Contract grant number: 3.4607.99.
Contract grant sponsor: Fondation David & Alice Van Buuren.

behavior. These results show how regulatory feedback processes at the cellular level allow the emergence of a coherent biological rhythm out of molecular noise. Int J Quantum Chem 98: 228–238, 2004

Key words: circadian rhythms; stochastic simulations; molecular noise; chaos; computational model

Introduction

How cohorts of innumerable molecules synchronize their dynamic behavior to produce periodic oscillations observable on a macroscopic level represents one of the most remarkable manifestations of self-organization in chemical kinetics. The work of Ilya Prigogine has shown that such oscillatory phenomena correspond to the evolution toward a temporal dissipative structure that occurs beyond a critical point of instability of a nonequilibrium steady state; the oscillations originate from appropriate nonlinearities of the underlying kinetic equations and require energy dissipation for their maintenance [1]. If oscillations are well known in a number of chemical reactions, the question arises as to why periodic behavior is so common in biological systems. The main reasons are that living organisms are open systems that operate far from thermodynamic equilibrium, and are subjected to a variety of regulatory processes that introduce nonlinearities, which favor the occurrence of periodic behavior [2].

The evolutionary pressure that acts on living systems has allowed the development of such regulations, which serve to optimize the functioning of unicellular or multicellular organisms, hence the profusion of rhythmic phenomena that are encountered at all levels of biological organization. Thus, in single cells, oscillations can occur with periods ranging from milliseconds to 24 h, depending on the type of regulatory mechanism involved in generating the cellular rhythm. The fastest rhythms rely on the regulation of ion channels in electrically excitable cells, while slower rhythms originate from the regulation of gene expression.

Most living organisms have developed the capability of generating autonomously sustained oscillations with a period close to 24 h. These oscillations, known as circadian rhythms, are endogenous because they can occur in constant environmental conditions, e.g., constant darkness [3]. Circadian rhythms can be entrained by light–dark cycles, allowing living organisms to adapt to the natural periodicity of their environment. The prominence of circadian oscillations is such that they form the core subject of chronobiology, the study of biological rhythms.

The molecular bases of circadian rhythms represent a topic of key importance for comprehending the dynamics of cellular processes and the physiology of living organisms. Experimental studies during the past decade have shed much light on the molecular mechanism of circadian rhythms. Initial studies pertained to the fungus *Neurospora* [4] and the fly *Drosophila* [5]. Molecular studies of circadian rhythms have since been extended to cyanobacteria, plants, and mammals [4–7]. In all cases investigated so far, the molecular mechanism of circadian oscillations relies on the negative autoregulation exerted by a protein on the expression of its gene [4–8]. Thus, in *Drosophila*, the proteins PER and TIM form a complex that indirectly represses the activation of the *per* and *tim* genes, while in *Neurospora* it is the FRQ protein that represses the expression of its gene *frq* [4–6]. The situation in mammals resembles that observed in *Drosophila*, but it appears that, instead of TIM, it is the CRY protein that forms a regulatory complex with a PER protein to inhibit the expression of the *per* genes [7]. Light can entrain circadian rhythms by inducing degradation of the TIM protein in *Drosophila*, and expression of the *frq* and *per* genes in *Neurospora* and mammals, respectively [4–7].

A number of mathematical models for circadian rhythms have been proposed [9–15] on the basis of these experimental observations. These models are of a deterministic nature and take the form of a system of coupled ordinary differential equations. The models predict that, in a certain range of parameter values, the genetic control network undergoes sustained oscillations of the limit cycle type corresponding to the circadian rhythm, whereas outside this range the gene network operates in a stable steady state.

The question arises as to whether deterministic models are always appropriate for the description of circadian clocks [16]. Indeed, the number

of molecules involved in the regulatory mechanism producing circadian rhythms at the cellular level may well be reduced. This number could vary from a few thousands down to hundreds and even a few tens of protein or messenger RNA molecules in each rhythm-producing cell. At such low concentrations, it is more appropriate to resort to a stochastic approach to study the molecular bases of the oscillatory phenomenon. Molecular fluctuations can be taken into account by describing the chemical reaction system as a birth-and-death stochastic process governed by a master equation [17]. In a given reaction step, molecules of participating species are either produced (birth) or consumed (death). At each step is associated a transition probability proportional to the numbers of molecules of involved chemical species and to the chemical rate constant of the corresponding deterministic model. A numerical algorithm that implements such a master equation approach to stochastic chemical dynamics was introduced by Gillespie [18, 19]. We shall use stochastic simulations to test the robustness of circadian rhythms with respect to fluctuations, and to investigate the progressive emergence of a biological rhythm out of the disorder of molecular noise.

Deterministic and Stochastic Versions of the Core Model for Circadian Oscillations

In a previous publication [20] we compared the stochastic and deterministic versions of a core molecular model for circadian oscillations based on the negative regulation exerted by a protein on the expression of its gene. To perform stochastic simulations, we resorted to the Gillespie algorithm [18, 19], after decomposing the deterministic model into elementary steps. We studied the effect of molecular noise by assessing the robustness of circadian oscillations as a function of the number of interacting molecules. We showed that robust circadian rhythmicity can occur when the maximum numbers of mRNA and clock protein molecules are in the tens and hundreds, respectively. Cooperativity of repression and periodic forcing by light–dark cycles enhance the robustness of circadian oscillations. In subsequent work [21, 22], we compared two stochastic versions of this core model: one fully developed into elementary steps, and the other nondeveloped. We showed that stochastic treatment of these two versions of the model for circadian rhythms yield similar results.

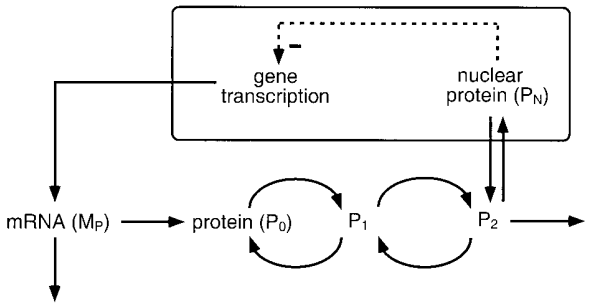

FIGURE 1. Scheme of the deterministic five-variable core model considered for circadian oscillations, with indication of parameters characterizing the different steps [9, 10]. The model is based on the repression exerted by the nuclear form of a clock protein (P_N) on the transcription of its gene into mRNA (M_P). mRNA is synthetized in the nucleus and transferred to the cytosol, where it accumulates at a maximum rate v_s; there it is degraded by an enzyme of maximum rate v_m and Michaelis constant K_m. The rate of synthesis of the protein P_0, proportional to M_P, is characterized by an apparent first-order rate constant k_s. Parameters v_i and K_i (i = 1,...,4) denote the maximum rate(s) and Michaelis constant(s) of the kinase and phosphatase involved in the reversible phosphorylation of P_0 into P_1 and P_1 into P_2, respectively. The fully phosphorylated form P_2 is degraded by an enzyme of maximum rate v_d and Michaelis constant K_d, and is transported into the nucleus at a rate characterized by the apparent first-order rate constant k_1. Transport of the nuclear form of the clock protein (P_N) into the cytosol is characterized by the apparent first-order rate constant k_2. The negative feedback exerted by the nuclear clock protein on gene transcription is described by an equation of the Hill type, in which n denotes the degree of cooperativity, and K_I the threshold constant for repression.

The model, schematized in general form in Figure 1, is based on the negative feedback exerted by a protein (referred to below as clock protein) on the expression of its gene. The deterministic version of this model, previously proposed for circadian oscillations of the PER protein and *per* mRNA in *Drosophila*, accounts for the occurrence of sustained oscillations in continuous darkness, phase-shifting by light pulses, and entrainment by light–dark cycles. Similar results have been obtained in more detailed models incorporating additional clock gene products such

as TIM and CLOCK [11–15]. However, for simplicity, we will focus on the model based on the regulation exerted by PER alone. The model of Figure 1 can thus serve as a core model capable of generating circadian oscillations, and does not aim at representing the current, more complex view of the molecular mechanism of the *Drosophila* and mammalian circadian clocks, which is known to involve a larger number of interacting proteins [5–7]. In this simple form, the model also applies to the case of *Neurospora* [3], where circadian rhythms originate from the negative feedback exerted by the FRQ protein on the expression of its gene.

In the deterministic version of the model schematized in Figure 1, the temporal variation of the concentrations of mRNA (M_P) and of the various forms of clock protein, cytosolic (P_0, P_1, P_2) or nuclear (P_N), is governed by the following system of five kinetic equations [9, 10, 20]:

$$\frac{dM_P}{dt} = \nu_s \frac{K_I^n}{K_I^n + P_N^n} - \nu_m \frac{M_P}{K_m + M_P}$$

$$\frac{dP_0}{dt} = k_s M_P - \nu_1 \frac{P_0}{K_1 + P_0} + \nu_2 \frac{P_1}{K_2 + P_1}$$

$$\frac{dP_1}{dt} = \nu_1 \frac{P_0}{K_1 + P_0} - \nu_2 \frac{P_1}{K_2 + P_1} - \nu_3 \frac{P_1}{K_3 + P_1} + \nu_4 \frac{P_2}{K_4 + P_2}$$

$$\frac{dP_2}{dt} = \nu_3 \frac{P_1}{K_3 + P_1} - \nu_4 \frac{P_2}{K_4 + P_2} - \nu_d \frac{P_2}{K_d + P_2} - k_1 P_2 + k_2 P_N$$

$$\frac{dP_N}{dt} = k_1 P_2 - k_2 P_N \qquad (1)$$

The stochastic version of the model was studied by means of the numerical algorithm introduced by Gillespie [18, 19], which implements a master equation approach to stochastic chemical dynamics [17]. This approach has previously been followed for studying the effect of noise on chemical oscillations [23, 24]. The Gillespie method associates a probability with each reaction; at each time step, the algorithm stochastically determines the reaction that takes place according to its probability, as well as the time interval to the next reaction. The numbers of molecules of the different reacting species, as well as the probabilities, are updated at each time step. In this approach a parameter denoted Ω permits the modulation of the number of molecules present in the system [18, 19].

To assess the effect of molecular noise on circadian oscillations, we used this method to perform stochastic simulations of the core deterministic model described above, after decomposing it into a detailed reaction system consisting of 30 elementary steps [20]. These steps are listed in Table I below, with the probability of their occurrence, denoted w_i (i = 1, …, 30). Each w_i is the product of a rate constant times the number(s) of molecules involved in the reaction step. Because each enzymatic reaction is fully decomposed into elementary steps, enzyme–substrate complexes are considered explicitly. The detailed reaction system thus contains 22 variables instead of 5 in the deterministic model. In Table I, the central column shows the reaction steps involving the indicated molecular species, with the rate constant indicated above the arrow. In the right column, showing the probability of occurrence of the various reaction steps, italicized capitals denote the numbers of molecules of the corresponding species involved in the particular reaction step.

Steps (1–8) pertain to the formation and dissociation of the various complexes between the gene promoter and nuclear protein (P_N). G denotes the unliganded promoter of the gene, while GP_N, GP_{N2}, GP_{N3}, and GP_{N4} denote the complexes formed by the gene promoter with 1, 2, 3, or 4 P_N molecules. Step (9) relates to the active state of the promoter leading to expression of the gene and synthesis of mRNA (M_P). In the case considered we assume that only the complex between the promoter and four molecules of P_N is inactive. Steps (10–12) pertain to the degradation of M_P by enzyme E_m, through formation of the complex C_m. Step (13) relates to synthesis of unphosphorylatyed clock protein (P_0) at a rate proportional to the number of mRNA molecules. Steps (14–16) refer to the phosphorylation of P_0 into P_1 by kinase E_1, through formation of complex C_1. Steps (17–19) refer to the dephosphorylation of P_1 into P_0 by phosphatase E_2, through the formation of complex C_2. Steps (20–25) pertain to the corre-

TABLE I

Decomposition of the core deterministic model of Fig. 1 into detailed reaction steps.*

Reaction no.	Reaction step	Probability of reaction
1	$G + P_N \xrightarrow{a_1} GP_N$	$w_1 = a_1 \times G \times P_N/\Omega$
2	$GP_N \xrightarrow{d_1} G + P_N$	$w_2 = d_1 \times GP_N$
3	$GP_N + P_N \xrightarrow{a_2} GP_{N2}$	$w_3 = a_2 \times GP_N \times P_N/\Omega$
4	$GP_{N2} \xrightarrow{d_2} GP_N + P_N$	$w_4 = d_2 \times GP_{N2}$
5	$GP_{N2} + P_N \xrightarrow{a_3} GP_{N3}$	$w_5 = a_3 \times GP_{N2} \times P_N/\Omega$
6	$GP_{N3} \xrightarrow{d_3} GP_{N2} + P_{N3}$	$w_6 = d_3 \times GP_{N3}$
7	$GP_{N3} + P_N \xrightarrow{a_4} GP_{N4}$	$w_7 = a_4 \times GP_{N3} \times P_N/\Omega$
8	$GP_{N4} \xrightarrow{d_4} GP_{N3} + P_N$	$w_8 = d_4 \times GP_{N4}$
9	$[G, GP_N, GP_{N2}, GP_{N3}] \xrightarrow{\nu_s} M_P$	$w_9 = \nu_s \times (G + GP_N + GP_{N2} + GP_{N3})$
10	$M_P + E_m \xrightarrow{k_{m1}} C_m$	$w_{10} = k_{m1} \times M_P \times E_m/\Omega$
11	$C_m \xrightarrow{k_{m2}} M_P + E_m$	$w_{11} = k_{m2} \times C_m$
12	$C_m \xrightarrow{k_{m3}} E_m$	$w_{12} = k_{m3} \times C_m$
13	$M_P \xrightarrow{k_s} M_P + P_0$	$w_{13} = k_s \times M_P$
14	$P_0 + E_1 \xrightarrow{k_{11}} C_1$	$w_{14} = k_{11} \times P_0 \times E_1/\Omega$
15	$C_1 \xrightarrow{k_{12}} P_0 + E_1$	$w_{15} = k_{12} \times C_1$
16	$C_1 \xrightarrow{k_{13}} P_1 + E_1$	$w_{16} = k_{13} \times C_1$
17	$P_1 + E_2 \xrightarrow{k_{21}} C_2$	$w_{17} = k_{21} \times P_1 \times E_2/\Omega$
18	$C_2 \xrightarrow{k_{22}} P_1 + E_2$	$w_{18} = k_{22} \times C_2$
19	$C_2 \xrightarrow{k_{23}} P_0 + E_2$	$w_{19} = k_{23} \times C_2$
20	$P_1 + E_3 \xrightarrow{k_{31}} C_3$	$w_{20} = k_{31} \times P_1 \times E_3/\Omega$
21	$C_3 \xrightarrow{k_{32}} P_1 + E_3$	$w_{21} = k_{32} \times C_3$
22	$C_3 \xrightarrow{k_{33}} P_2 + E_3$	$w_{22} = k_{33} \times C_3$
23	$P_2 + E_4 \xrightarrow{k_{41}} C_4$	$w_{23} = k_{41} \times P_2 \times E_4/\Omega$
24	$C_4 \xrightarrow{k_{42}} P_2 + E_4$	$w_{24} = k_{42} \times C_4$
25	$C_4 \xrightarrow{k_{43}} P_1 + E_4$	$w_{25} = k_{43} \times C_4$
26	$P_2 + E_d \xrightarrow{k_{d1}} C_d$	$w_{26} = k_{d1} \times P_2 \times E_d/\Omega$
27	$C_d \xrightarrow{k_{d2}} P_2 + E_d$	$w_{27} = k_{d2} \times C_d$
28	$C_d \xrightarrow{k_{d3}} E_d$	$w_{28} = k_{d3} \times C_d$
29	$P_2 \xrightarrow{k_1} P_N$	$w_{29} = k_1 \times P_2$
30	$P_N \xrightarrow{k_2} P_2$	$w_{30} = k_2 \times P_N$

*Steps 1–8 have been developed for the case $n = 4$. Only steps 1–6, 1–4, and 1–2 must be considered if the maximum number of P_N molecules binding to the gene promoter is equal to 3, 2, or 1.

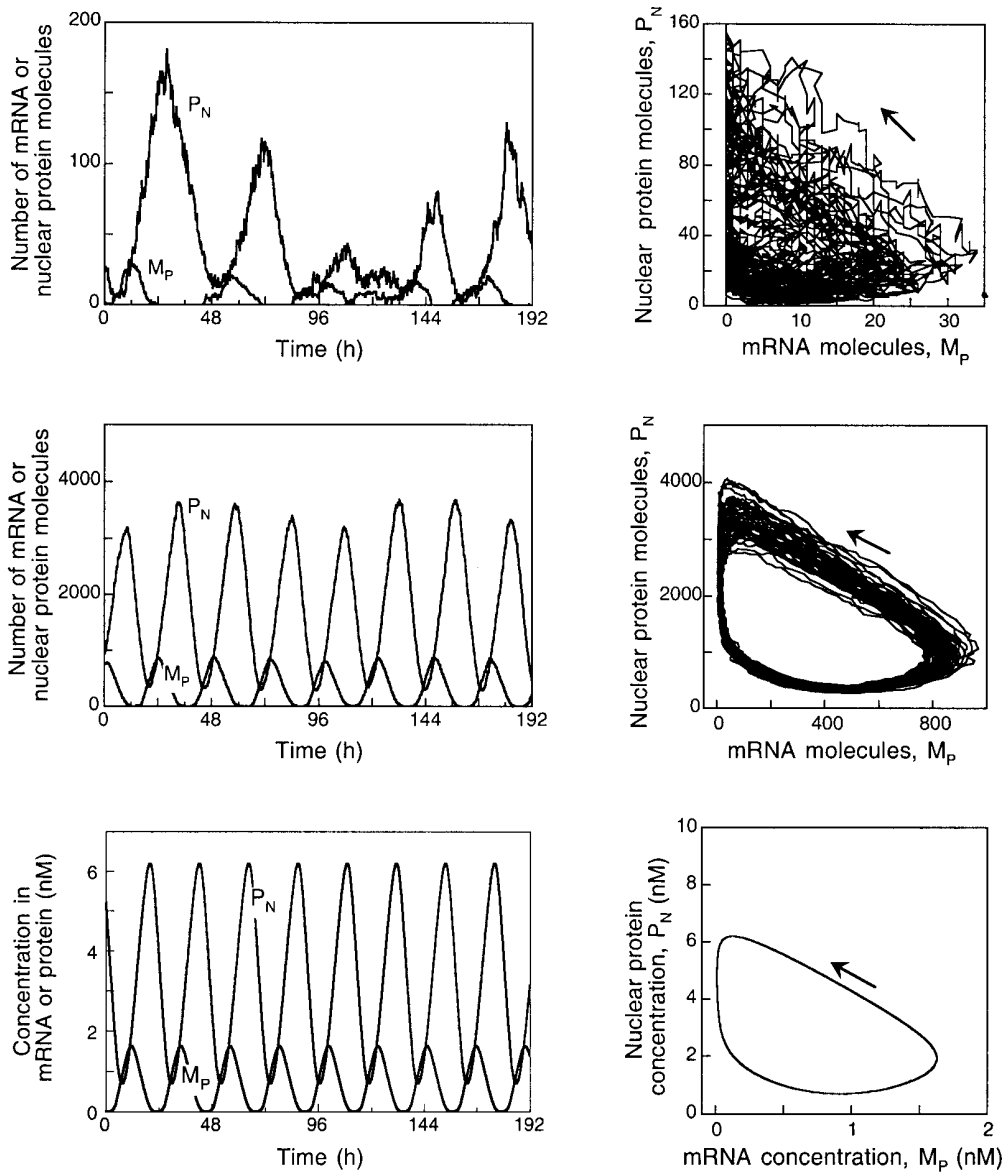

FIGURE 2. Sustained oscillations (left column) and limit cycle (right column) predicted by the deterministic and stochastic versions of the model for circadian rhythms. Bottom row: Sustained oscillations of mRNA (M_P) and nuclear clock protein (P_N) obtained in the five-variable deterministic model governed by Eq. (1) and corresponding limit cycle shown as a projection onto the M_P-P_N phase plane; the arrow indicates the direction of movement along the closed trajectory. Top and middle panels: limit cycle and sustained oscillations (represented by the time course of the number of mRNA and nuclear clock protein molecules) predicted by the stochastic model for values of parameter Ω increasing from 10 (upper row) to 500 (middle row). The results, obtained in the presence of molecular noise, should be compared with those obtained with the deterministic model (bottom row). Stochastic simulations were performed by means of the Gillespie method [18, 19] with the model listed in Table I. Parameter values for deterministic and stochastic simulations are given in Appendix in ref. 20 (see http://www.pnas.org/cgi/content/full/022628299/DC1).

sponding phosphorylation of P_1 into P_2 and dephosphorylation of P_2 into P_1. Steps (26–28) relate to the degradation of the phosphorylated form P_2 by enzyme E_d, through formation of complex C_d. Steps (29) and (30) refer, respectively, to entry of P_2 into and exit of P_N from the nucleus.

Instead of decomposing the deterministic model into elementary steps (developed model), nonlinear kinetic functions (e.g., Michaelis–Menten expressions, or the repression function given by an expression of the Hill type) can simply be included in the probabilities associated with the global reaction steps (nondeveloped model). The developed and nondeveloped versions of the stochastic model for circadian rhythms yield similar results [21, 22].

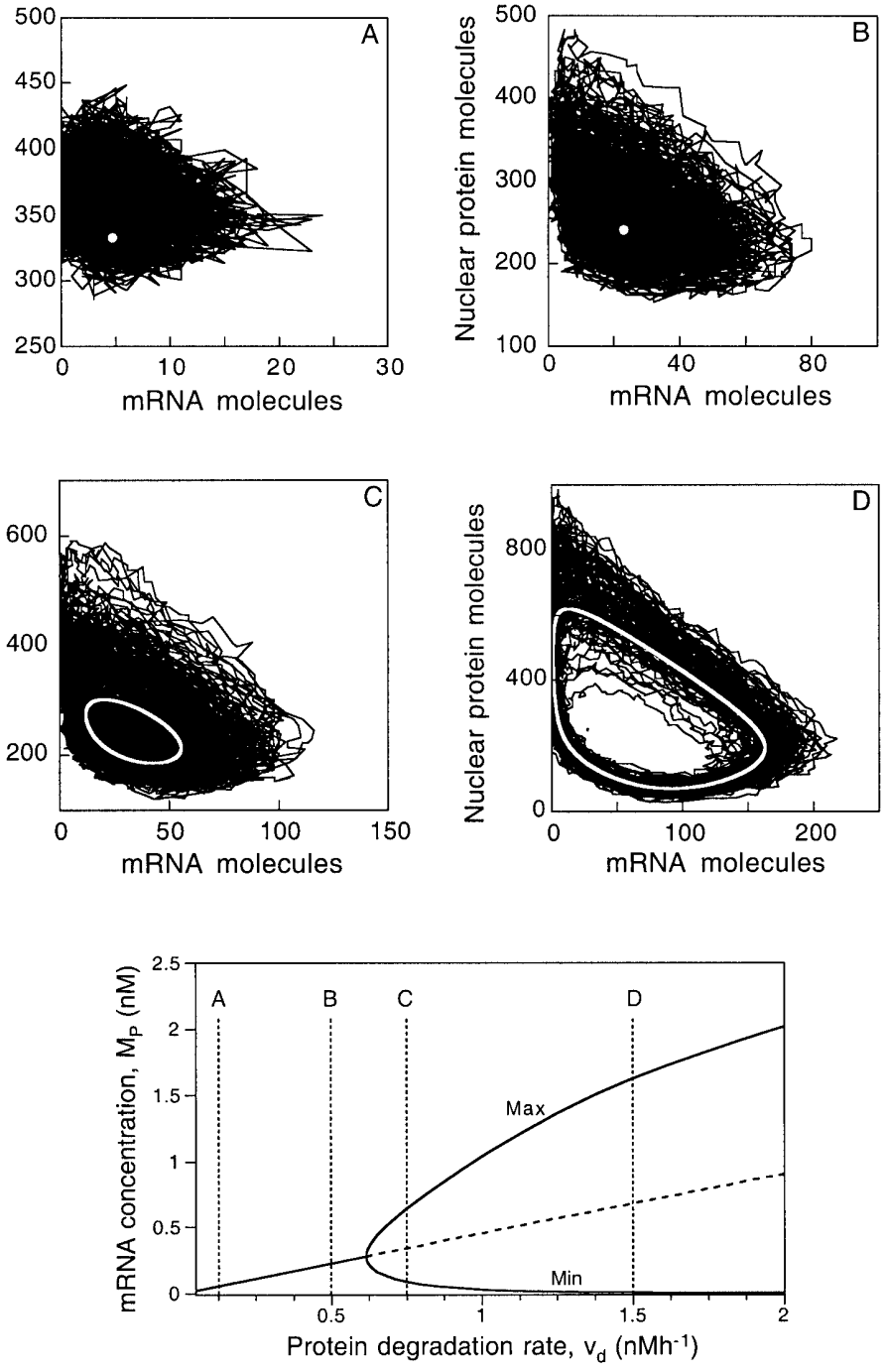

FIGURE 3.

Emergence of Periodic Oscillations From Molecular Noise

For appropriate parameter values, the deterministic model predicts the occurrence of sustained oscillations (Fig. 2, bottom left), which correspond to the evolution toward a closed curve, known as a limit cycle, in the phase plane (Fig. 2, bottom right). The typical oscillatory behavior of the five-variable system is illustrated by the time evolution of the concentrations of mRNA (M_P) and of nuclear clock protein (P_N).

Can these predictions of deterministic oscillatory behavior be recovered when resorting to stochastic simulations? Figure 2 (top and middle rows) shows the results of such simulations of the core model for circadian rhythms performed for $\Omega = 10$ and 500, respectively. Figure 2 (left column) shows the time evolution of two variables of the model, the numbers of molecules (or concentrations; Fig. 2, bottom row) of mRNA (M_P) and of nuclear clock protein (P_N). When the maximum numbers of molecules of mRNA and nuclear protein are small, of the order of 30 and 150, respectively ($\Omega = 10$), the effect of molecular noise is important. Nevertheless, repetitive peaks of nuclear protein are clearly discernible (left, upper), but these oscillations are highly irregular. The corresponding trajectory in the phase plane (top right) takes the form of a highly noisy limit cycle. For larger values of Ω, the oscillations are much more regular (middle left). In the case considered ($\Omega = 500$), the values of the maximum numbers of molecules are much higher, of the order of 800 and 4000 for the mRNA and nuclear protein, respectively. The corresponding limit cycle is closely related to the corresponding deterministic trajectory (bottom right). The noisy limit cycle possesses a certain thickness, particularly noticeable along the branch going from the maximum in mRNA to the maximum in nuclear protein.

Thus, stochastic simulations show that even when the maximum numbers of molecules remain reduced, of the order of a few tens and a few hundreds for the mRNA and nuclear protein, the deterministic approach provides a faithful picture of the onset of circadian oscillations. The agreement between the stochastic and deterministic approaches increases with the value of Ω, i.e., with the number of molecules participating in the oscillatory mechanism.

In the deterministic model, sustained oscillations occur when a parameter exceeds a critical bifurcation value. This is illustrated in Figure 3 (bottom) in the bifurcation diagram established as a function of parameter v_d, which measures the rate of degradation of the clock protein. The diagram shows the steady state concentration of mRNA, which is either stable (solid line) or unstable (dashed line), as a function of v_d. In Figure 3A–D, the white dot or white curve shows the steady state or limit cycle predicted in the phase plane by the deterministic model for the corresponding parameter values (A–D) in the bifurcation diagram. The four diagrams thus correspond to the four v_d values indi-

FIGURE 3. Effect of the proximity from a bifurcation point on the effect of molecular noise in the stochastic model for circadian rhythms. (A–D) Results of deterministic (white dot or curve) or stochastic simulations (black curves) of trajectories followed in the phase plane for the four increasing values of parameter v_d corresponding to those shown in the bifurcation diagram (bottom panel) : 0.2 (A), 0.5 (B), 0.7 (C), and 1.5 (D); these values, to be multiplied by $\Omega = 100$, are expressed here in molecules per h. The following situations are illustrated in the four panels: (A) Fluctuations around a stable steady state. (B) Fluctuations around a stable steady state for a value of v_d close to the bifurcation point; damped oscillations occur in these conditions when the system is displaced from the stable steady state. The white dot (A, B) represents the stable steady state predicted by the deterministic version of the model in corresponding conditions. (C) Oscillations observed close to the bifurcation point. (D) Oscillations observed further from the bifurcation point, well into the domain of sustained oscillations. The thick white curve (C, D) represents the limit cycle predicted by the deterministic version of the model governed by Eq. (1), in corresponding conditions, for the same values of v_d expressed in nMh^{-1}. The smaller amplitude of the limit cycle in (C) as compared to the limit cycle in (D) is associated with an increased influence of molecular noise. The stochastic curves are obtained by means of the Gillespie algorithm applied to the model of Table I (see refs. 20–22). Bottom: Bifurcation diagram established for the deterministic version of the model of Figure 1 as a function of parameter v_d (in nM/h), which measures the maximum rate of the clock protein degradation. The curve shows the steady-state level of mRNA, stable (solid line) or unstable (dashed line), as well as the maximum and minimum concentration of mRNA in the course of sustained circadian oscillations. The vertical dashed lines refer to the four values considered for v_d in A–D, respectively. The diagram is established by means of the program AUTO [29] applied to Eq. (1). Parameter values are as listed in refs. 21 and 22.

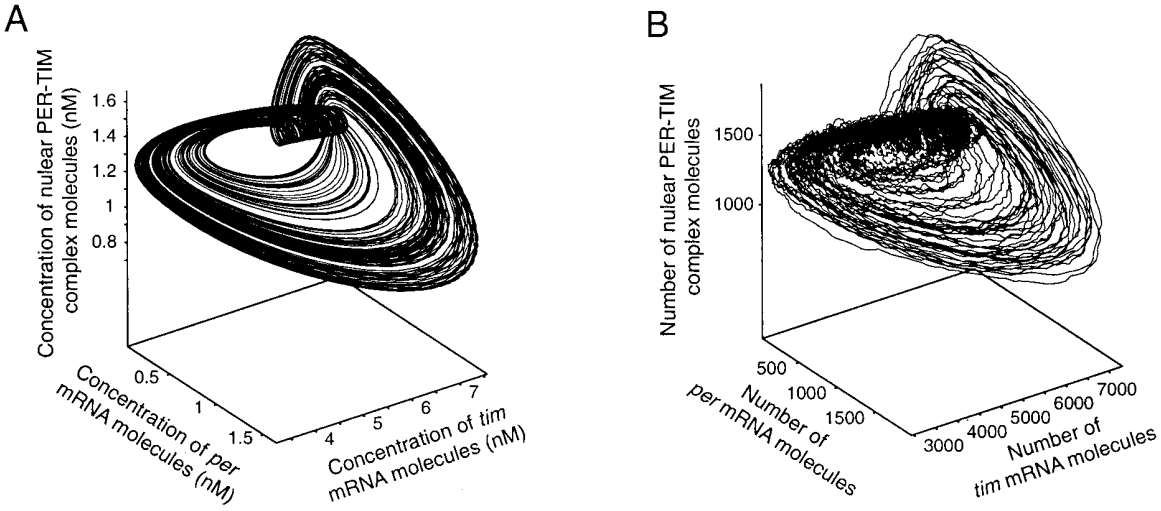

FIGURE 4. Effect of molecular noise on autonomous chaos. The strange attractor predicted [26] by the 10-variable deterministic model for circadian rhythms (A) is recovered in (B) by stochastic simulations [22].

cated by dashed vertical lines in Figure 3 (bottom). The corresponding results of stochastic simulations for $\Omega = 100$ are superimposed on the predictions from the deterministic model.

In Figure 3A, the deterministic system evolves to a stable steady state far from the bifurcation point; stochastic simulations show low-amplitude fluctuations around the deterministic steady state. In Figure 3B the deterministic system evolves to a stable steady state close to the bifurcation point; stochastic simulations show fluctuations of larger amplitude around the deterministic steady state. Just beyond the bifurcation point (Fig. 3C), the deterministic system undergoes limit cycle oscillations of reduced amplitude; stochastic simulations show low-amplitude noisy oscillations around the deterministic limit cycle, which resemble the fluctuations shown in Figure 3B. Finally, in the middle of the oscillatory domain, far from the bifurcation point (Fig. 3D), the deterministic system undergoes limit cycle oscillations of large amplitude; stochastic simulations show large-amplitude, relatively less noisy oscillations around the deterministic limit cycle.

The data presented in Figure 3 further confirm that stochastic simulations allow us to recover the dynamics predicted by the deterministic model. Below a critical parameter value the system displays low-amplitude fluctuations around a stable steady state, while above this value sustained oscillations occur. Moreover, the effect of fluctuations is enhanced by the proximity from the bifurcation point.

As previously done for model chemical reaction systems [25], stochastic simulations can also be used to study the occurrence of chaos in the presence of molecular noise in models for circadian oscillations [22]. We have previously reported the occurrence of autonomous chaos in an extension of the model shown in Figure 1 [26]. This extended 10-variable model was previously proposed for circadian oscillations of the PER and TIM proteins and of *per* and *tim* mRNAs in *Drosophila* [11, 12]. The model is based on the negative feedback exerted by the complex between the nuclear PER and TIM proteins on the expression of their genes. Although the physiological significance of chaotic behavior remains an open question within the context of circadian rhythms, its occurrence in a model for circadian oscillations allows us to assess the effect of molecular noise on chaos in a realistic model based on genetic regulation.

For some parameter values, in conditions corresponding to continuous darkness, sustained aperiodic oscillations occur in the extended model [26], which correspond to the evolution toward a strange attractor in the phase space (Fig. 4A). For $\Omega = 1000$, Figure 4B shows the results of stochastic simulations performed for parameter values corresponding to those producing chaos in the deterministic model in Figure 4A. The results indicate that chaos persists in the presence of noise, even though the structure of the strange attractor begins to be

blurred when the number of molecules decreases and the amplitude of fluctuations rises. Nevertheless the small curler-like substructure that characterizes the strange attractor in the (Fig. 4A) is clearly visible in the attractor obtained by stochastic simulations (Fig. 4B).

To compare the effect of molecular noise on periodic and chaotic oscillations we have used elsewhere Poincaré sections [22]. For the case of periodic oscillations, instead of a single point obtained with deterministic simulations, stochastic simulations yield a cloud of points surrounding the deterministic Poincaré section; the smaller the number of molecules, the more scattered the cloud. In the case of chaos, instead of a single point the intersection in the deterministic model takes the form of an open continuous curve. Stochastic simulations produce a cloudy version of this curve; the scattering of the points in this cloud increases as the number of molecules decreases [22]. The use of Poincaré sections thus leads to a clear distinction between noisy limit cycle oscillations and chaotic oscillations subjected to noise.

Concluding Remarks

Circadian rhythms represent a prototype of temporal self-organization in biological systems. These rhythms originate from the negative autoregulation of gene expression. Deterministic models based on such regulatory processes have been proposed for circadian rhythms in *Drosophila* and *Neurospora*. However, when numbers of participating molecules are reduced and molecular noise becomes significant, the question arises as to whether genetic control mechanisms can give rise to coherent circadian oscillations at the cellular level [16]. In the presence of reduced numbers of molecules of the mRNA and protein species involved in the circadian clock mechanism, this issue must be addressed by means of stochastic simulations [20].

The stochastic approach shows that as in the deterministic case, sustained oscillations can occur when control parameters pass critical values (Fig. 3). At first, just beyond the bifurcation point, when the amplitude of the deterministic limit cycle is small, the effect of molecular noise is important and fluctuations prevent the emergence of regular periodic behavior (Fig. 3C). Once the system operates far from the bifurcation point, well into the domain of sustained oscillations, a coherent rhythm emerges as periodic behavior overcomes the dampening effect of molecular noise (Fig. 3D).

The study of the stochastic version of a core model for circadian oscillations based on negative autoregulation of a clock gene by its protein product further indicates that robust circadian oscillations, comparable to those predicted by the deterministic approach, can occur even when the maximum numbers of mRNA and clock protein molecules are in the tens and hundreds, respectively. The robustness of circadian rhythms, quantified by the period distribution and the half-time of the autocorrelation function [20], is enhanced when the cooperativity of the repression process increases and when the numbers of mRNA and protein molecules involved in the oscillatory mechanism become larger. These numerical results were corroborated by a recent analytical study [27]. Stochastic simulations indicate, moreover, that forcing by a light–dark cycle stabilizes the phase of the oscillations [20].

Autonomous chaos has previously been described in the deterministic PER-TIM model for circadian rhythms in *Drosophila* [26]. As for periodic circadian oscillations, chaotic behavior is recovered when stochastic simulations are performed for parameter values corresponding to chaos in the deterministic model. Beyond a noisy appearance attributable to fluctuations in the presence of reduced numbers of mRNA and protein molecules, the structure of the strange attractor remains discernible (Fig. 4) in agreement with results obtained in models for chemical oscillations [25, 28]. The agreement between the stochastic and deterministic approaches therefore holds for periodic oscillations, as well as for chaotic behavior. Even in the presence of relatively small numbers of participating molecules, of the order of only tens or hundreds, periodic or chaotic oscillations can readily overcome molecular noise. The case of circadian rhythms exemplifies how regulatory feedback loops giving rise to nonequilibrium instabilities are associated with the emergence of oscillatory behavior. Stochastic simulations allow us to grasp the very onset of a coherent biological rhythm out of molecular noise.

ACKNOWLEDGMENTS

A. G. acknowledges the continuing support of the late Professor Ilya Prigogine, whose enthusiasm and inspirational views had a profound impact on his research on the physicochemical bases of biological rhythms. This work was supported by grant

3.4607.99 from the Fonds de la Recherche Scientifique Médicale (F. R. S. M., Belgium). Support from the Fondation David & Alice Van Buuren to D. G. is also acknowledged.

References

1. Prigogine, I. Introduction to Thermodynamics of Irreversible Processes. Wiley: New York, 1967.
2. Prigogine, I. In Theoretical Physics and Biology; Marois, M., Ed.; North-Holland: Amsterdam, 1969; p 23–52.
3. Moore-Ede, M. C.; Sulzman, F. M., Fuller, C. A. The Clocks That Time Us. Physiology of the Circadian Timing System. Harvard University Press: Cambridge, MA, 1982.
4. Dunlap, J. C. Cell 1999, 96, 271–290.
5. Williams, J. A.; Sehgal, A. Annu Rev Physiol 2001, 63, 729–755.
6. Young, M. W.; Kay, S. A. Nature Rev Genet 2001, 2, 702–715.
7. Reppert, S. M.; Weaver, D. R. Annu Rev Physiol 2001, 63, 647–676.
8. Hardin, P. E.; Hall, J. C.; Rosbash M. Nature 1990, 343, 536–540.
9. Goldbeter, A. Proc R Soc Lond B 1995, 261, 319–324.
10. Goldbeter, A. Biochemical Oscillations and Cellular Rhythms. The Molecular Bases of Periodic and Chaotic Behaviour; Cambridge University Press: Cambridge, UK, 1996.
11. Leloup, J. C.; Goldbeter, A. J. Biol. Rhythms 1998, 13, 70–87.
12. Leloup, J. C.; Gonze, D., Goldbeter, A. J Biol Rhythms 1999, 14, 433–448.
13. Leloup, J. C.; Goldbeter, A. BioEssays 2000, 22, 84–93.
14. Ueda, H. R.; Hagiwara, M.; Kitano, H. J Theor Biol 2001, 210, 401–406.
15. Smolen, P.; Baxter, D. A.; Byrne J. H. J Neurosci 2001, 21, 6644–6656.
16. Barkai, N.; Leibler, S. Nature 2000, 403, 267–268.
17. Nicolis, G.; Prigogine, I. Self-Organization in Nonequilibrium Systems; Wiley: New York, 1977.
18. Gillespie, D. T. J Comput Phys 1976, 22 403–434.
19. Gillespie, D. T. J Phys Chem 1977, 81, 2340–2361.
20. Gonze, D.; Halloy, J.; Goldbeter, A. Proc Natl Acad Sci USA 2002, 99, 673–678.
21. Gonze, D.; Halloy, J.; Goldbeter, A. J Biol Phys 2002, 28, 637–653.
22. Gonze, D.; Halloy, J.; Leloup, J. C.; Goldbeter A. C R Biol 2003, 326, 189–203.
23. Baras, F.; Pearson, J. E.; Malek Mansour, M. J Chem Phys 1990, 93, 5747–5750.
24. Baras, F. In Stochastic Dynamics. Lecture Notes in Physics; LNP484; Schimansky-Geier L.; Poeschel T., Eds.; Springer-Verlag: Berlin, 1997; p 167–178.
25. Geysermans, P.; Baras, F. J Chem Phys 1996, 105, 1402–1408.
26. Leloup, J. C.; Goldbeter, A. J Theor Biol 1999, 198,445–459.
27. Gonze, D.; Halloy, J.; Gaspard P. J Chem Phys 2002, 116, 10997–11010.
28. Peeters, P.; Nicolis, G. Physica A 1992, 188, 426–435.
29. Doedel, E. J. Congr Num 1981, 30, 265–284.